

AD-A173 734

DEFORMATION OF RAPIDLY SOLIDIFIED TI-2ER(U)  
PENNSYLVANIA STATE UNIV UNIVERSITY PARK DEPT OF  
MATERIALS SCIENCE AND ENGINEERING S L KAMPE ET AL.

1/1

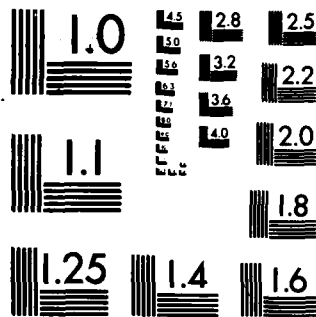
UNCLASSIFIED

SEP 86 TR-3 N00014-86-K-0301

F/G 11/6

NL





MICROCOPY RESOLUTION TEST CHART  
NATIONAL BUREAU OF STANDARDS-1963-A

12

AD-A173 734

TECHNICAL REPORT NO. 3

TO

THE OFFICE OF NAVAL RESEARCH  
CONTRACT No. N00014-86-K-0381

DTIC  
SELECTE  
NOV 06 1986  
S D D

DEFORMATION OF RAPIDLY SOLIDIFIED Ti-2Er

S. L. KAMPE<sup>+</sup> AND D. A. KOSS<sup>\*</sup>

<sup>+</sup>DEPARTMENT OF METALLURGICAL ENGINEERING  
MICHIGAN TECHNOLOGICAL UNIVERSITY  
HOUGHTON, MI 49931

<sup>\*</sup>DEPARTMENT OF MATERIALS SCIENCE AND ENGINEERING  
THE PENNSYLVANIA STATE UNIVERSITY  
UNIVERSITY PARK, PA 16802

DTIC FILE COPY

REPRODUCTION IN WHOLE OR IN PART IS PERMITTED  
FOR ANY PURPOSE OF THE UNITED STATES GOVERNMENT.  
DISTRIBUTION OF THIS DOCUMENT IS UNLIMITED.

**DISTRIBUTION STATEMENT A**  
Approved for public release;  
Distribution Unlimited

86 11 6 062

REPORT DOCUMENTATION PAGE		READ INSTRUCTIONS BEFORE COMPLETING FORM
1. REPORT NUMBER 3	2. GOVT ACCESSION NO.	3. RECIPIENT'S CATALOG NUMBER <b>AD-A173734</b>
4. TITLE (and Subtitle) Deformation of Rapidly Solidified Ti-2Er		5. TYPE OF REPORT & PERIOD COVERED
7. AUTHOR(s) S. L. Kampe and D. A. Koss		6. PERFORMING ORG. REPORT NUMBER
9. PERFORMING ORGANIZATION NAME AND ADDRESS Dept. Materials Science and Eng. The Pennsylvania State University University Park, PA 16802		8. CONTRACT OR GRANT NUMBER(s)
11. CONTROLLING OFFICE NAME AND ADDRESS Office of Naval Research 800 N. Quincy St. Arlington, VA 22217		10. PROGRAM ELEMENT, PROJECT, TASK AREA & WORK UNIT NUMBERS
14. MONITORING AGENCY NAME & ADDRESS (if different from Controlling Office)		12. REPORT DATE Sept. 1986
		13. NUMBER OF PAGES 7
		15. SECURITY CLASS. (of this report) Unclassified
16. DISTRIBUTION STATEMENT (of this Report)  Distribution of this document is unlimited.		15a. DECLASSIFICATION/DOWNGRADING SCHEDULE
17. DISTRIBUTION STATEMENT (of the abstract entered in Block 20, if different from Report)		
18. SUPPLEMENTARY NOTES		
19. KEY WORDS (Continue on reverse side if necessary and identify by block number) Deformation, Temperature, Creep, rapid solidification, dispersion hardening, titanium alloys.		
20. ABSTRACT (Continue on reverse side if necessary and identify by block number) The deformation of rapidly solidified Ti-2Er has been studied over a range of temperatures from ambient to 775°C. When compared to the behavior of Ti tested under parallel conditions, the results indicate that although dispersion strengthening occurs, its magnitude is dependent on temperature, strain rate, and grain size. Minimal strengthening is observed in fine grained material at high temperatures, low stresses and strain rates. This behavior, combined with microstructural observations using transmission electron microscopy, indicates a susceptibility to grain boundary sliding at elevated temperatures.		

## DEFORMATION OF RAPIDLY SOLIDIFIED Ti-2Er

S. L. Kampe<sup>†</sup> and D. A. Koss<sup>\*</sup>

<sup>†</sup>Department of Metallurgical Engineering  
Michigan Technological University  
Houghton, MI 49931

<sup>\*</sup>Department of Materials Science and Engineering  
The Pennsylvania State University  
University Park, PA 16802

### Abstract

The deformation of rapidly solidified Ti-2Er has been studied over a range of temperatures from ambient to 775°C. When compared to the behavior of Ti tested under parallel conditions, the results indicate that although dispersion strengthening occurs, its magnitude is dependent on temperature, strain rate, and grain size. Minimal strengthening is observed in fine grained material at high temperatures, low stresses and strain rates. This behavior, combined with microstructural observations using transmission electron microscopy, indicates a susceptibility to grain boundary sliding at elevated temperatures.

RAPID SOLIDIFICATION (RS) techniques have been recently applied to titanium-based alloys designed for high temperature use. These alloys are based on the introduction of a fine, homogeneous dispersion of oxide particles through the internal oxidation of rare-earth alloying additions to the titanium matrix. Several investigators have established the potential of RS in oxide dispersion strengthened (ODS) titanium alloy development through extensive evaluation of the thermal-mechanical stability of candidate microstructures (see, for example, REF. 1-7). In this regard, microstructural studies, as well as hardness measurements on aged RS Ti alloys in the as-quenched form of ribbons or flakes, have indicated improved microstructural stability and the potential for high temperature strengthening in several alloy systems based on rare earth elemental additions to a titanium matrix.

However, commercial application of titanium

based alloys produced via rapid solidification will rely not only on the retention of favorable microstructural features but also on enhanced creep strength following consolidation of the fine-scaled RS product into bulk, useable form. The consolidation processing relies primarily on powder metallurgy techniques, typically involving hot isostatic pressing (HIP) and/or hot extrusion to achieve full density in a manner which will result in minimal microstructural degradation.

Despite numerous studies of the microstructural stability of various RS Ti alloys in ribbon form, there has been no systematic study of the high temperature creep behavior of an ODS titanium alloy formed by RS and consolidated into bulk form. Only a few data are available, and these indicate strengthening over a narrow range of stress/temperature/strain rates (5). The present work explores the microstructural evolution and subsequent deformation behavior of rapidly solidified commercially pure (CP) Ti alloyed with 2 w/o Er which has been consolidated into bulk form. As a basis for comparison, the behavior of this alloy is compared to dispersoid-free CP Ti with the same grain size. Included in this study will be data describing the deformation behavior as a function of temperature, strain rate, and grain size.

### EXPERIMENTAL DETAILS

**CONSOLIDATION PROCESSING** - Rapidly solidified Ti-2Er, supplied by Dr. S.H. Whang of New York Polytechnic University, was fabricated in the form of 25-50  $\mu$ m thick ribbon using a continuous feed, melt spinning apparatus, as described elsewhere (7). The ribbon was pressed to a 100% dense, bulk form by the following sequence: (a) the as-quenched ribbon was pressed into a decar-

burized steel can to approximately 85% of theoretical density, (b) the packed can was evacuated to less than  $2 \times 10^{-4}$  Pa and hermetically sealed, (c) the evacuated can was HIPped under conditions of moderate consolidation temperature and high pressure (800°C/207 MPa/4 hrs), and (d) the HIP can was removed by machining and the resulting compact inserted into a protective stainless steel jacket and extruded at a temperature of 700 °C at an extrusion ratio of 7:1. Following hot extrusion, the stainless steel jacket was removed by machining, leaving a fully dense, consolidated product in the form of 4.0 mm diameter rod. Prior to testing and microstructural observation, the as-processed alloy was annealed at 775°C for 2 hours to relieve residual stresses due to extrusion. In order to obtain a larger grain size in this alloy, it was necessary to heat treat within the beta phase field ( $T > 882^\circ\text{C}$ ). A 2 hour, 932°C beta anneal, followed by 24 hours at 775°C, resulted in an average grain size increase from 4 to 25  $\mu\text{m}$ . All heat treatments were performed in a vacuum of at least  $2 \times 10^{-4}$  Pa.

As a basis of comparing the deformation behavior of the ODS material to a dispersion-free counterpart, compacts of CP titanium powder were prepared. The powder was initially cold isostatically pressed (400 MPa), sintered (1400°C, 4 hours), swaged (75% RA), and annealed (500°C, 4 hours) to produce a fully dense, recrystallized microstructure with a 4  $\mu\text{m}$  grain size equal to that of the as-processed RS Ti-2Er. A 25  $\mu\text{m}$  average grain size was obtained with an additional anneal at 800°C for 2 hours. Table I summarizes the processing history and the resulting oxygen analyses for each alloy prior to subsequent testing but after processing.

MECHANICAL TESTING - Slow strain-rate compression testing was performed at temperatures of 20, 300, 600, 700, and 775°C at engineering strain rates of  $5.0 \times 10^{-5}$ ,  $2.5 \times 10^{-4}$ ,  $1.25 \times 10^{-3}$ , and  $6.25 \times 10^{-3}$  /s. Right-cylinder compression specimens were machined to a diameter of approximately 4 mm and to a height of 10.7 mm ( $h_0/d_0 = 8/3$ ). To avoid alloy contamination during elevated temperature exposure, testing was performed in a sealed atmosphere chamber, evacuated and backfilled with flowing, high purity argon prior to and during testing.

#### RESULTS AND DISCUSSION

The as-consolidated microstructure of Ti-2Er is illustrated in Fig. 1. Several features are to be noted: (a) many very fine dispersoids (average diameter  $\approx 40$  nm) are present; these reside generally within the interior of the grain, (b) a few very large dispersoids (average diameter  $\approx 450$  nm) are also present; these are usually located on the grain boundaries, and (c) the titanium matrix possesses a very fine grain size, approximately 4  $\mu\text{m}$  average grain size. Prolonged heat treatments at temperatures below the beta transus (882°C) indicate that these microstructural features are extremely stable; no discernible coarsening occurs within the alpha-phase microstructure.

Fig. 2 illustrates the microstructure of the RS Ti-2Er alloy following the beta anneal for 2 hrs at 932°C. Two microstructural changes are evident. The average grain size has increased to approximately 25  $\mu\text{m}$  and the average dispersoid diameter has increased to approximately 300 nm. The very fine dispersoids are no longer present following the beta anneal.

Table I. Summary of Processing Conditions for CP Ti and Ti-2Er

Alloy	Grain size	Processing	O(wt %)	Er(wt %)
CP Ti	4 $\mu\text{m}$	Cold isostatic press (400 MPa) Vacuum sinter (1400°C, 4 hours) Swage (75 % RA) Vacuum anneal (500°C, 4 hours)	0.166	---
	25 $\mu\text{m}$	As above, plus vacuum anneal (800°C, 2 hours)		
Ti-2Er	4 $\mu\text{m}$	Hydraulic compaction, HIP (800°C/207 MPa/4 hr), Hot extrusion (700°C/7:1), and Vacuum anneal (775°C/2 hr)	0.080	1.97
	25 $\mu\text{m}$	As above, plus beta anneal (932°C/2 hr/775°C/24 hr)		



Name and Title

Date

A-1



Fig. 1 - TEM micrograph of the as-processed microstructure of the RS Ti-2Er alloy.



Fig. 2 - TEM micrograph of the RS Ti-2Er alloy following the beta grain growth anneal.

The dependence of the yield stress on test temperature for both the CP Ti and the RS Ti-2Er alloys is shown in Fig. 3. The figure includes data for material of 4 and 25 μm grain size and is based on a 0.2% offset definition of the yield stress. As seen in Fig. 3, the yield stresses decrease rapidly with temperature. Both fine-grained microstructures exhibit slightly superior strength at lower temperatures compared to the coarse-grain alloys. At higher temperatures, the

fine-grain Ti-2Er possesses inferior strength when compared to its coarse grain counterpart. No grain size effect is observed for the CP Ti for the conditions in the present study.

The results of the high temperature deformation testing over a range of strain rates are shown in Fig. 4. This Dorn-type plot illustrates the relationship between temperature, strain-rate (or near steady-state creep rate), and flow stress (near steady-state creep stress). For

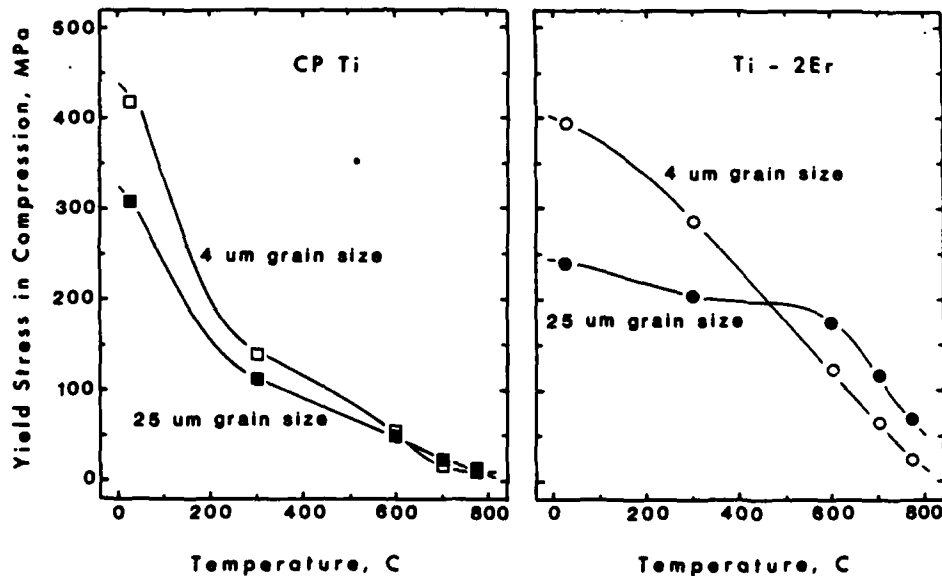


Fig. 3 - Yield stress as a function of temperature and grain size for CP Ti and consolidated RS Ti-2Er tested at a strain rate of  $2.5 \times 10^{-4}$  /s.

this study, the diffusion-compensated strain rate is plotted as function of modulus compensated flow stress. Both the diffusion coefficient (8), and elastic modulus (9) have been corrected for temperature. Specifically, this diagram is a compilation of data for CP Ti and Ti-2Er tested at 600, 700, and 775°C for grain sizes of 4 and 25  $\mu\text{m}$ . The dashed line represents the "best-fit" line obtained using data for CP Ti gathered from the literature by Doner and Conrad (10); these data show excellent agreement with the present results.

Several conclusions can be drawn from the results illustrated in Fig. 4. First, the dispersoid containing alloy, Ti-2Er, shows greater resistance to high temperature deformation than CP Ti at all temperatures, strain rates, and stresses tested. Secondly, the magnitude of the dispersion strengthening is very small at the combination of high temperature, low strain rates, and small grain sizes. Thirdly, increasing the grain size of the Ti-2Er alloy significantly enhances its high temperature creep resistance whereas no effect of grain size is observed for the CP titanium alloy.

Information regarding the predominating deformation mechanism can be obtained and/or es-

timated from Fig. 4. Nearly all general constitutive equations for high temperature deformation have the form (11):

$$\dot{\epsilon} = A (D_i/d^p) (\sigma/E)^n \quad \text{Eq. (1)}$$

- where  $\dot{\epsilon}$  = strain rate (usually a steady state creep rate)  
 A = structure sensitive constant independent of grain size  
 $D_i$  = diffusion coefficient, with the subscript i referring to the operative diffusion mechanism  
 d = grain size  
 p = grain size exponent, usually 0, 2, or 3  
 $\sigma$  = flow stress (usually a steady state flow stress)  
 E = elastic modulus  
 n = stress exponent, a constant whose value is dependent on the deformation mechanism operative

Thus for a Dorn-type plot as in Fig. 4, A and n may be calculated respectively from the intercept and slope of the resulting curve. Based on this type of analysis, Doner and Conrad concluded that dislocation creep (n = 5) dominates deformation of CP Ti in this region of stress and temperature; they conclude that the climb of dislocations past obstacles, such as other dislocations, is rate limiting. On the basis of the data in Fig. 4, such a conclusion is also consistent and reasonable for the present data, including that for conditions of low temperatures, high stresses, and/or high strain rates.

At high temperatures, low stresses, and/or low strain rates, the mechanism controlling the deformation of the RS Ti-2Er alloy changes, as indicated by the change in the slope or stress exponent for the Ti-2Er data in Fig. 4. In particular, the marked decrease in stress exponent at  $\dot{\epsilon}/D(T)$  values of less than  $10^{12} \text{ m}^{-2}$  suggests that grain boundary sliding may be contributing significantly to the overall deformation of the ODS alloy. Walser and Sherby (12) have summarized the constitutive equations for power law creep, and report three mechanisms which involve grain boundary sliding as a contributing and/or dominate deformation mechanism. These equations are given in Table II in the general form of Eq. (1). The equations predict that strain rate increases with decreasing grain size, specifically  $\dot{\epsilon} \propto d^{-2}$  or  $d^{-3}$ . Additionally, a stress exponent of 2 is typically observed for grain boundary sliding, and can be associated with continuum accommodation via lattice or grain

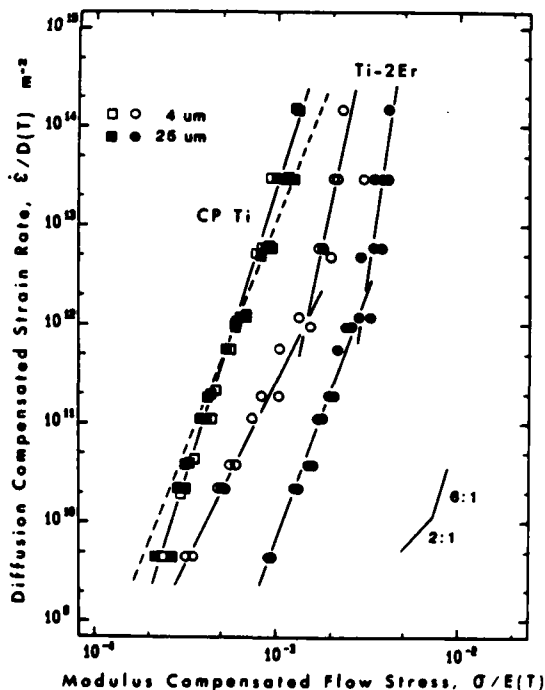


Fig. 4 - Near steady state strain rate as a function of stress for CP Ti and Ti-2Er for grain sizes of 4 and 25  $\mu\text{m}$ .

Table II. Grain Boundary Sliding Constitutive Equations for Creep of Polycrystalline Metals, from Walser and Sherby (11)

Accommodation mechanism	Constitutive equation
Lattice diffusion	$\dot{\epsilon} = 2 \times 10^9 (D_L/d^2) (\sigma/E)^2$
Grain boundary diffusion	$\dot{\epsilon} = 1 \times 10^8 (D_B/d^3) (\sigma/E)^2$
Pipe diffusion	$\dot{\epsilon} = 2 \times 10^{11} (D_P/d^2) (\sigma/E)^4$

boundary diffusion. However, stress exponents of 4 have also been reported for grain boundary sliding under conditions of intermediate stresses, intermediate temperatures, and fine grain sizes. This large exponent has been predicted and explained in terms of a large contribution from pipe diffusion as an accommodation mechanism.

Fig. 5 illustrates the data for the Ti-2Er as compensated for an  $\dot{\epsilon} \propto d^{-2}$  dependence of strain rate on grain size. As shown, the data for both grain sizes fall approximately along a single line, obeying a constitutive equation (in the form of Eq. (1)) of

$$\dot{\epsilon} = 6 \times 10^{11} (D_i/d^2) (\sigma/E)^{3.9} \quad \text{Eq. (2)}$$

Comparing Eq. (2) with the constitutive equations for grain boundary sliding in Table II indicates good agreement with a grain boundary sliding/pipe diffusion mechanism controlling the rate of deformation. In any event, noting the inverse dependence of the strain rate on the square of the grain size, we can reasonably conclude that some form of grain boundary sliding is a dominant deformation mechanism for fine grain RS Ti-2Er.

The question arises as to why the introduction of the dispersoids induce grain boundary sliding in this titanium alloy. Fundamental to oxide dispersion strengthening design strategies is the assumption that the thermally stable dispersoids will act to inhibit creep-type deformation mechanisms, such as grain boundary sliding. To understand this apparent discrepancy, one must note that the dispersoids in the as-processed Ti-2Er are located almost entirely within grains; see Fig. (1). The primary effect of these dispersoids would be to strengthen the grain interiors, leaving the grain boundaries essentially unaffected. Thus, as is common in Ti alloys, this ODS Ti alloy can exhibit an appreciable degree of grain boundary sliding under the appropriate conditions. Following a grain growth anneal, improved high temperature strength is obtained primarily as a result of increasing grain size and secondly as a consequence of an increased density of of large dispersoids resid-

ing on the grain boundaries, thereby inhibiting grain boundary motion. This observation has considerable implications for the design of RS ODS titanium alloys for high temperature applications. To achieve maximum benefit from the oxide dispersion, processing must evolve a microstructure which is not only fully dense, homogeneous, and thermally stable, but one that will minimize or eliminate grain boundary sliding, especially at high temperatures, low stresses and strain rates.

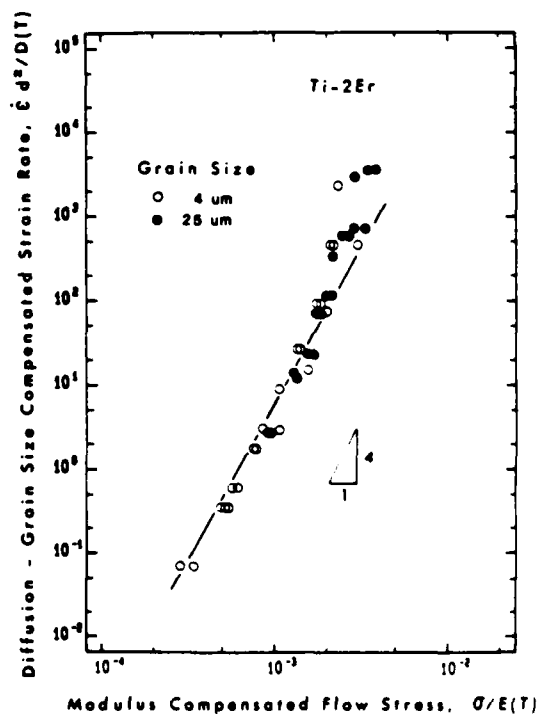


Fig. 5 - Diffusion - grain size compensated strain rate as a function of modulus compensated flow stress for RS Ti-2Er.

## CONCLUSIONS

1.) When consolidated to bulk form, rapidly solidified Ti-2Er exhibits oxide dispersion strengthening under conditions of high temperature deformation. However, the strengthening increment is sensitive to grain size, temperature, and strain rate such that minimal strengthening is observed at small grain sizes, high temperatures, and low strain rates.

2.) The near steady-state creep rate of the Ti-2Er depends on grain size such that  $\dot{\epsilon} \propto d^{-2}$ . Thus the creep resistance is enhanced considerably by a high temperature beta grain growth anneal even though the dispersoid particles coarsen considerably (from  $\approx 40$  nm to  $\approx 300$  nm) during the grain growth anneal.

3.) Analysis of the data suggests that dislocation climb past obstacles controls the deformation of the CP Ti and the Ti-2Er at low temperatures, high stresses, and high strain rates. At high temperatures, low stresses, and low strain rates, grain boundary sliding prevails as the dominating deformation mechanism for the Ti-2Er.

## ACKNOWLEDGEMENTS

The authors wish to thank Dr. Michael Gigliotti and Mr. Lee Perocchi of the General Electric Research Laboratory for their advice and assistance in the consolidation processing of the RS alloys. This research was supported by the Office of Naval Research through Contract No. N00014-86-K-0381.

## REFERENCES

1. H.B. Bomberger and F.H. Froes, Titanium, Rapid Solidification Technology (Proc Conf), New Orleans, March 2-6, 1986, 21-43.
2. S.H. Whang, J. Mat. Sci., 21, 1986, 2224-2238.
3. S.M.L. Sastry, D.M. Bowden, and R.J. Lederich, Titanium Science and Technology (Proc Conf), Vol. 1, Munich, Sept. 10-14, 1984, 435-441.
4. D.G. Konitzer, B.C. Muddle, H.F. Fraser, and R. Kirchheim, ibid., 405-410.
5. S.M.L. Sastry, P.J. Meschter, and J.E. O'Neal, Met Trans A, 15A, 1984, 1465-1484.
6. S.M.L. Sastry, T.C. Peng, P.J. Meschter, and J.E. O'Neal, J. Metals, 35 (9), 1983, 21-28.
7. S.H. Whang, J. Metals, 36 (4), 1984, 34-40.
8. P.M. Sargent and M.F. Ashby, Scr. Metall., 16, 1982, 1415-1422.
9. G. Simmons and H. Wang, Single Crystal Elastic Constants and Calculated Aggregate Properties: A Handbook, 2nd Ed., M.I.T. Press, 1971.
10. M. Doner and H. Conrad, Met. Trans, 4, 1973, 2809-2817.
11. O.D. Sherby and P.M. Burke, Progress in Mat. Sci., 13 (7), 1968, 325-390.
12. B. Walser and O.D. Sherby, Scr. Metall., 16, 1982, 213-219.

END

12-86

DTIC